Research Article

Journal of Environmental Nanotechnology

Biogenic Silver Nanoparticles from *Manilkara zapota* and *Curcuma longa*: Characterization and Biomedical Activities

Steffy Dominic[1], Perumal Elumalai[2], Rajeshkumar Shanmugam[3*] and Nalini Jeyaprakash[1]

[1]Department of Physiology, Saveetha Medical College and Hospital, Saveetha Institute of Medical and Technical Sciences, Saveetha University, Chennai, TN, India

[2]Department of Biochemistry, Saveetha Medical College and Hospital, Saveetha Institute of Medical and Technical Sciences, Saveetha University, Chennai, TN, India

[3]Department of Anatomy, Saveetha Medical College and Hospital, Saveetha Institute of Medical and Technical Sciences, Saveetha University, Chennai, TN, India

Received: 25.06.2026 Accepted: 26.07.2026 Published: 30.09.2026

*rajeshkumars.sdc@saveetha.com

ABSTRACT

The study aimed to develop silver nanoparticles (AgNPs) using herbal formulations from *Manilkara zapota* and *Curcuma longa* and to evaluate their biomedical applications. AgNPs were synthesized using an aqueous leaf extract prepared from *Manilkara zapota* and *Curcuma longa* and characterized using UV–Vis spectroscopy, SEM, FTIR, and XRD. Antioxidant activity was assessed by the 2,2-diphenyl-1-picrylhydrazyl (DPPH), hydrogen peroxide (H_2O_2), ferric reducing antioxidant power (FRAP), 2,2′-azino-bis(3-ethylbenzothiazoline-6-sulfonic acid) (ABTS), and nitric oxide (NO) assays and compared with the standard ascorbic acid, while anti-inflammatory potential was assessed by BSA, egg albumin, and MSA assays and compared with the standard diclofenac sodium. Antibacterial activity was evaluated by the agar-well diffusion method and time–kill curve assay against wound pathogens. The generation of silver nanoparticles (AgNPs) was validated through UV–Vis spectral analysis, which showed a peak at 435 nm. The DPPH, H_2O_2, FRAP, ABTS, and NO assays showed concentration-dependent inhibition, with a maximum at 50 µg/mL. Similarly, the BSA, egg albumin, and MSA assays demonstrated concentration-dependent effects, with maximum anti-inflammatory potential at 50 µg/mL. The agar-well diffusion and time–kill curve assays demonstrated the antibacterial potential of AgNPs against wound pathogens, with inhibition zones of 14 mm for *Escherichia coli,* 18 mm for *Pseudomonas* sp., 16 mm for *Staphylococcus aureus,* and 9 mm for *Candida albicans*. This study demonstrates an eco-friendly preparation of AgNPs using a combined leaf extract of *M. zapota* and *C. longa*, along with their significant antioxidant and anti-inflammatory potential. In addition, the AgNPs exhibited antibacterial activity against wound pathogens. The results support the use of silver nanoparticles in therapeutic applications.

Keywords: Silver nanoparticles; Green synthesis; Antibacterial activity; Antioxidant activity; Anti-inflammatory activity.

1. INTRODUCTION

Nanotechnology has emerged as a crucial tool in biomedicine, enabling advanced biosensing platforms and imaging technologies, as well as tissue engineering and drug delivery systems (Singh and Lillard, 2009). Nanoparticles are nanoscale particles ranging between 10 and 1000 nm that possess physicochemical properties (Khan *et al.* 2019). Nanoparticle–based targeted drug delivery systems exhibit specificity and therapeutic efficacy of bioactive molecules (Singh and Lillard, 2009).

Among various nanoparticles, silver nanoparticles (AgNPs) have unique size-, electrical-, and shape-dependent optical and antimicrobial properties. AgNPs can be synthesized through several methods, including physical and chemical methods that provide size precision but pose ecological and biological hazards. Plant-mediated green synthesis is a promising alternative to conventional synthesis because it can reduce the use of hazardous reagents and may offer an eco-friendly and cost-effective route for nanoparticle production (Iravani *et al.* 2014; Pauline *et al.* 2025; Varadharajan and Pandian, 2025). AgNPs showed significant bactericidal efficacy against both *S. aureus* and *E. coli*, confirming broad-spectrum antimicrobial potential through ROS (Reactive Oxygen Species) generation and membrane disruption, concentration-dependent cytotoxic activity against cancer cells, and promising anticancer potential (Abdulsahib, 2021). *Syzygium aromaticum*-derived AgNPs show potent anti-inflammatory activity in both *in vitro* and *in silico* analyses by inhibiting inflammatory cytokines IL-1β and stabilizing membranes. *In silico* analysis reinforced these observations, highlighting the synergistic effect of the plant molecules and AgNPs (Varghese *et al.* 2017) and antidiabetic activity by suppressing α-amylase and α-glucosidase activity (Balan *et al.* 2016).

Manilkara zapota, also known as sapodilla or chikko, belongs to the Sapotaceae family, has significant medicinal value, and has been used to treat ailments such as cold, cough, diarrhea, indigestion, and pyrexia (Rivas-Gastelum *et al.* 2023); it also shows anti-inflammatory and antioxidant activity (Gomathy *et al.* 2013). These activities enhance the wound-healing potential of *Manilkara zapota*. A study shows that a topical ointment from its bark extract has significant wound-healing potential *in vitro* and *in vivo* (Alsareii *et al.* 2023). A previous study by Lekkala *et al.* (2025) observed a concentration-dependent antioxidant potential of green-synthesized AgNPs using *Tinospora cordifolia*, with DPPH inhibition of 10, 18, 22, and 31% at 25, 50, 75, and 100 µg/mL, respectively (Lekkala *et al.* 2025). Similarly, a study reported that plant-mediated silver nanoparticles from *Saussurea obvallata* demonstrated antioxidant and antimicrobial activity, with 61.21±0.02% DPPH radical scavenging at 500 µg/mL and inhibition zones of 12 and 13 mm against *E. coli* and *E. faecalis*, respectively (Sagar *et al.* 2024).

Curcuma longa, widely known as turmeric, is a perennial herb belonging to the Zingiberaceae family (Wickenberg *et al.* 2010). Traditionally, *Curcuma longa* has been used to treat colds, stomachache, jaundice, wounds, arthritis, skin infections, diarrhea, liver disorders, and menstrual disorders. It has also been used to treat asthma, anemia, bronchitis, fever, dysentery, and diabetes (Subedi, 2019). It has also been reported to exhibit anti-inflammatory (Chainani-Wu, 2003) and antioxidant (Choi *et al.* 2020) activities. Furthermore, *Curcuma longa* is used as an anticancer agent, with molecular docking showing that Curcuma longa bioactives, such as curcumin, demethoxycurcumin, and bisdemethoxycurcumin, interfere with oncogenic and immune-inflammatory pathways, particularly PI3K-AKT, MAPK, and IL-17, suppressing tumor-promoting inflammation and enhancing apoptosis (Li and Li, 2022). Recent studies have highlighted that the unique phytochemical composition of *Manilkara zapota*, such as polyphenols and flavonoids, functions as a natural reducing and stabilizing agent; these results are responsible for the reduction and formation of stabilized AgNPs (Sahu *et al.* 2024). Similarly, the bioactive compound curcumin, present in *Curcuma longa*, serves as a reducing and capping agent and has also been shown to enhance antibacterial properties (Shahraki *et al.* 2026). The ethanolic extract of *Curcuma longa* contains abundant flavonoids and polyphenols, which are responsible for its remarkable antioxidant potential (Grover *et al.* 2021). Another study found that AgNPs from turmeric extract exhibited enhanced antioxidant activity compared with the standard ascorbic acid (Selvan *et al.* 2018). Majani *et al.* (2025) found that biogenic synthesis of silver nanoparticles (AgNPs) mediated by *Manilkara zapota* plant extract involves reducing silver ions (Ag+) to metallic silver (Ag˚) through phytochemicals in the plant. Similarly, Parashar and Garg, (2023) synthesized AgNPs using *Manilkara zapota* fruit extract and concluded that polyphenolic compounds such as quercitrin, dihydromyricetin, methyl chlorogenate, and gallocatechin are associated with antimicrobial activity.

This study aims to synthesize silver nanoparticles using a combined leaf extract of *Manilkara zapota* and *Curcuma longa* and to evaluate their biomedical potential, antimicrobial efficacy, and cytotoxic activity. The study's novelty lies in integrating these phytochemical extracts to produce bioactive, green-synthesized silver nanoparticles with enhanced synthesis, biomedical efficacy, and stability. Overall, the findings show that the green synthesis of AgNPs provides a simple and eco-friendly method. The results demonstrate their potential for biomedical applications.

2. MATERIALS AND METHODS

2.1 Preparation of *Manilkara zapota* and *Curcuma longa* extract

The synthesis was performed in triplicate under identical experimental conditions. The leaves were thoroughly washed using tap water and distilled water, dried, and coarsely powdered. 0.5 g each of *Manilkara zapota* leaf powder and *Curcuma longa* leaf powder was added to 100 mL of purified water. The mixture was heated at 50 °C in a heating mantle for 15–20 min with gentle heating. The resulting extract was then filtered through a muslin cloth. Subsequently, 1 mM (0.051 g) of silver nitrate was dissolved in 80 mL of distilled water. Then, 1 mL of the prepared extract was transferred to a 100 mL Erlenmeyer flask and mixed with 2.5 mL of the silver nitrate solution. To observe the color change, the extract mixture was exposed to sunlight. The extract was centrifuged at 8000 rpm for 15 min and refrigerated in an airtight container for further investigation.

2.2 Preparation of *Manilkara zapota*- and *Curcuma longa*-mediated AgNPs

1mM silver nitrate ($AgNO_3$) solution is dissolved in 80 mL of distilled water. 20 mL of the prepared *Manilkara zapota* and *Curcuma longa* extract is mixed with the solution and magnetically stirred at 650–800 rpm for 72 h to reduce silver ions. The fabrication of silver nanoparticles was verified by the color change to dark brown (Fig. 1).

2.3 Biomedical Applications

2.3.1 Estimation of the Antioxidant Activity of AgNPs

H_2O_2 Assay

The hydrogen peroxide radical scavenging activity of the biosynthesized silver nanoparticles was determined. 1 mL of AgNPs at different concentrations

(10 µg/mL to 50 µg/mL) was placed in appropriately labeled test tubes and mixed with 200 µL (0.2 mL) of hydrogen peroxide. The test tubes were incubated in the dark for 10 min. The absorbance was measured at 532 nm.

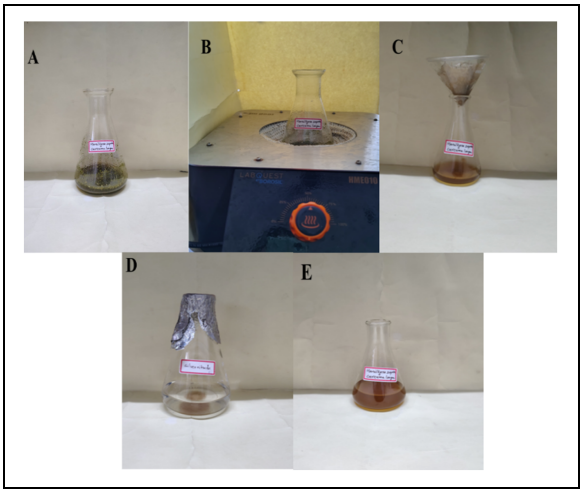

Fig. 1: Synthesis of AgNPs using *M. zapota* and *C. longa* extract: (A) *M. zapota* and *C. longa* extract, (B) boiling of *the* extract using a heating mantle, (C) filtration of the extract using muslin cloth, (D) silver nitrate solution and (E) *M. zapota* and *C. longa*-mediated AgNPs

DPPH Assay

The free radical inhibition of biosynthesized AgNPs was evaluated by the DPPH assay. 1 mL of biosynthesized AgNPs at different concentrations (10 µg/mL to 50 µg/mL) was added to appropriately labeled test tubes and mixed with 1 mL of 1 mM DPPH; the solution was then incubated in the dark at room temperature for up to 10 min. After incubation, the chromatic change of DPPH from purple to yellow was noted, and the spectroscopic absorbance value was recorded at 517 nm.

FRAP Assay

For the FRAP assay, 0.5 mL of ferric chloride was added to *Manilkara zapota*- and *Curcuma longa*-mediated AgNPs of different concentrations (10–50 µg/mL). Then, 2.5 mL phosphate buffer was added, followed by 2.5 mL potassium ferricyanide, and the mixture was incubated for 30 min. Samples were heated in a thermal bath for 10 min, then centrifuged.

A 2.5 mL portion of supernatant was collected, diluted with an equal amount of distilled water, and incubated for 10 min. Absorbance was measured at 700 nm.

ABTS Assay

The ABTS assay was performed by adding 250 µL of ABTS solution to a 96-well plate, then adding 20 µL of AgNP solution at varying concentrations (10 µg/mL–50 µg/mL), and incubating in the dark for 20 min. The absorbance was measured at 734 nm.

Nitric Oxide Assay

Nitric oxide scavenging activity was assessed by incubating a solution composed of 0.5 mL phosphate buffer, 2 mL sodium prusside and *Manilkara zapota* and *Curcuma longa*-mediated AgNPs in different concentrations (10–50 µg/mL) at 25 °C for 150 min. After incubation, 1 mL of sulfanilic acid was added to 0.5 mL of the AgNPs and kept for 5 min, followed by the addition of naphthylethylenediamine dihydrochloride; the solution was then incubated for 30 min in diffused light at 25 °C, and the development of a pink chromophore was observed. The absorbance of the developed color was measured at 540 nm.

2.3.2 Estimation of Anti-inflammatory Activity of AgNPs

Bovine Serum Albumin (BSA) Assay

The anti-inflammatory assays in this study followed protocols reported in previous studies (Dhanapal *et al.* 2025). The bovine serum albumin denaturation assay was utilized to determine the inflammation-suppressing activity of green-fabricated AgNPs. 1 mL of BSA was added to 1 mL of biosynthesized AgNPs at different concentrations (10 µg/mL to 50 µg/mL); the solution was then incubated in the dark at ambient temperature for 10 min after being heated on a heating mantle at 550 °C for 30 min. The absorbance exhibited a value of 660 nm.

Egg Albumin Assay

3 mL of egg albumin was mixed with 2.8 mL of freshly prepared 1X phosphate buffer used to determine the egg albumin denaturation assay. The different concentrations of green-synthesized silver nanoparticles (10 µg/mL to 50 µg/mL) were kept at room temperature for 10 min, then incubated in a thermostatic bath at 55 °C for 10 min. The adsorption was measured at 660 nm.

Membrane Stabilization (MSA) Assay

The MSA assay was utilized to further examine the anti-inflammatory property. Blood samples were collected in an anticoagulant-treated tube, centrifuged at 1000 rpm for 10 min, and RBCs were isolated and washed three times with phosphate-buffered saline (PBS); Tris-HCl buffer was used to prepare a 10% suspension. A measured 1 mL of suspension was treated with varying concentrations of AgNPs (10–50 µg/mL), incubated at 37 °C for 30 min, and analyzed at 540 nm.

Antimicrobial Activity

Antibacterial activity was performed using the Agar well diffusion method. About 100 mL of Mueller–

Hinton agar plates were aseptically swabbed with five clinically isolated *E. coli, Pseudomonas* sp., *E. faceium*, and *S. aureus*. For inoculation, four wells were made in each plate using a T-shaped well cutter. The test samples were added at concentrations of 25, 50, and 100 µg/mL, and a standard antibiotic was added as a control, followed by incubation at 37 °C for 24 h; antibacterial activity was quantified by the diameter of the clear zones. Antifungal activity against *C. albicans* was assessed on Rose Bengal Petri plates. After solidification, *C. albicans* was swabbed, and wells were made similarly; test samples (25, 50, and 100 µg/mL) and the standard antibiotic amoxicillin for bacteria and fluconazole for fungi were added. The plates were maintained at 37˚C for 48 h, and the zone of inhibition was recorded; the test was performed in triplicate for each microorganism.

Time–kill curve assay

The antibacterial potential of *Manilkara zapota*- and *Curcuma longa*-mediated AgNPs was investigated using the time–kill curve assay. Five pathogenic microorganisms, including *E. coli, E. faecium*, *Pseudomonas* sp., *S. aureus*, and *C. albicans,* were cultured in Mueller-Hinton broth and exposed to the AgNPs at concentrations of 25, 50, and 100 µg/mL, along with the standard antimicrobial control. 0.5 McFarland standard of tested pathogens was inoculated into sterile PBS and incubated on Mueller-Hinton agar plates at 37 °C for 24 h to reach the late log phase. Then, 30 mL of the inoculum was diluted with 15 mL of pre-heated Mueller-Hinton broth, and 90 µL of this mixture was added to each well of a 96-well ELISA.

3. STATISTICAL ANALYSIS

All experiments were performed in triplicate, and results are presented as mean ± standard deviation (SD). Statistical analysis was carried out using two–way ANOVA, with $p<0.0005$ regarded as statistically significant.

4. RESULTS AND DISCUSSION

This investigation evaluated the *Manilkara zapota*- and *Curcuma longa*-mediated AgNPs and their biomedical potential. The phytochemicals present in *C. longa*, including curcuminoids and terpenoids, play a significant role in anti-inflammatory, antioxidant, anticancer, antimicrobial, and antiseptic effects (Sharifi-Rad *et al.* 2020). The UV–Vis spectra of the synthesized AgNPs showed an absorption peak between 430–450 nm across all time intervals (12, 24, and 36 h). The absorption peak at 435 nm is characteristic of AgNPs and is associated with surface plasmon resonance, confirming AgNP formation. The absorption peak of green-synthesized AgNPs at 12 h was at 460 nm, which subsequently shifted to 455 nm at 24 h. At 36 h, the peak became more defined, confirming AgNP formation. The high absorbance peak at 36 h suggests AgNP formation in the synthesized solution. Metallic nanoparticles interact with the incident light; electromagnetic radiation induces free oscillation of free surface electrons, resulting in LSPR. The resulting band is influenced by nanoparticle shape, size, crystallinity, and aggregation state (Li *et al.* 2023). A study on the synthesis of AgNPs using *Ribes rubrum* berries reported a maximum absorbance at 435 nm (Rizwana *et al.* 2022). Another study reported a maximum absorbance peak at 420 nm of green-synthesized AgNPs using *Stachytarpheta indica* (Joshi *et al.* 2025). The UV–Vis spectra recorded at 12, 24, and 36 h showed a gradual increase in absorbance intensity without a noticeable shift in the SPR (surface plasmon resonance) peak, approximately 435–440 nm. The progressive peak indicates nanoparticle formation with continuous reduction of silver (Ag^+) ions (Ahmed *et al.* 2016).

The surface morphology of the green-synthesized AgNPs using combined leaf extract of *M. zapota* and *C. longa* was characterized using SEM analysis. The SEM micrographs revealed predominantly spherical to quasi-spherical AgNPs (Figs. 3A–C) with moderate aggregation, which is frequently observed in green-synthesized nanoparticles due to their high surface energy. The SEM images exhibited agglomerated spherical AgNPs derived from *C. longa* of 20–53 nm (Segneanu *et al.* 2022). Another study reported spherical AgNPs in the SEM micrographs and concluded that this shape is advantageous for biomedical applications.

The FTIR spectra (Fig. 4) support the involvement of phytochemical functional groups in the synthesis of AgNPs. The broad absorption peak at 3400 cm^{-1} indicates O-H stretching of phenolic compounds, which act as reducing and stabilizing agents and play a role in donating electrons to facilitate nanoparticle formation, while the peak at 2429.82 cm^{-1} represents C=O stretching in alkynes. The absorption band near 1635.29 cm^{-1} corresponds to C=C stretching (alkenes/amide groups), whereas a band at 1114 cm^{-1} represents C–N stretching. The band near 660.19 cm^{-1} indicates Ag–O stretching of esters/ethers. Additional peaks at 826.36 cm^{-1} and 661.74 cm^{-1} correspond to C–H stretching. Dibua and Ezeh (2025) reported similar findings, concluding that the FTIR spectrum confirmed the involvement of phytochemicals in the formation of *Plectranthus amboinicius*-mediated silver nanoparticles, which exhibited absorption peaks at 3400, 1630, 1384, 1108, and 620 cm^{-1} (Dibua and Ezeh, 2025).

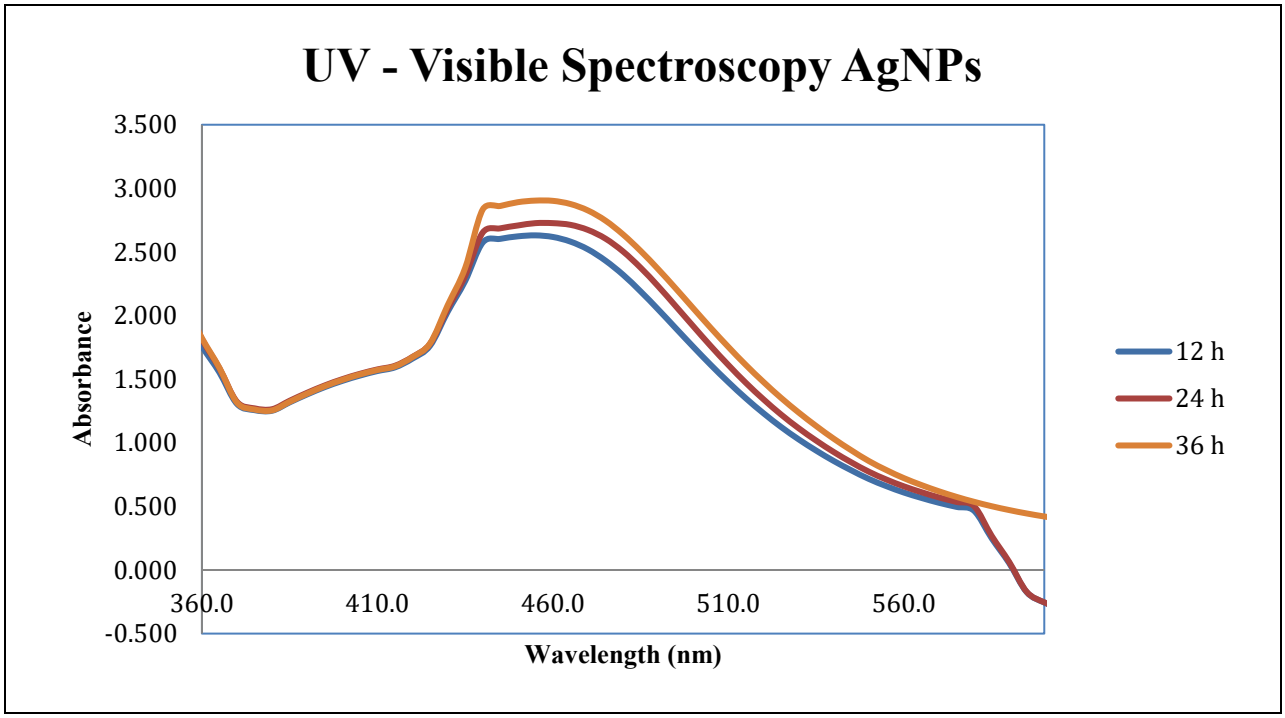

Fig. 2: UV–Vis spectra of green-synthesized AgNPs using *M. zapota* and *C. longa*

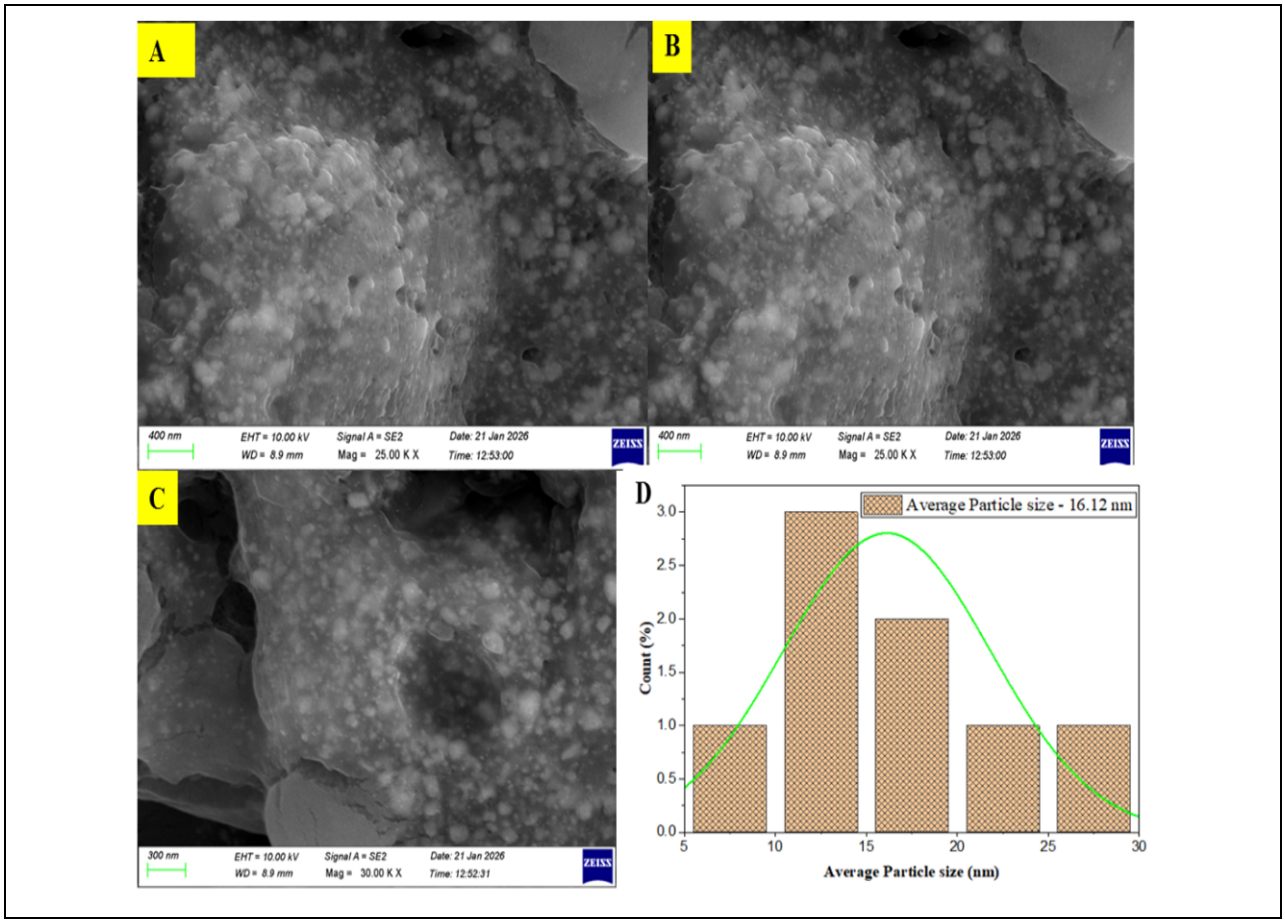

Fig. 3: SEM images of *M. zapota*- and *C. longa*-mediated AgNPs at different scale-bar sizes: (A–B) 400 nm, (C) 300 nm and (D) size distribution histogram of the AgNPs (average size = 16.12 nm)

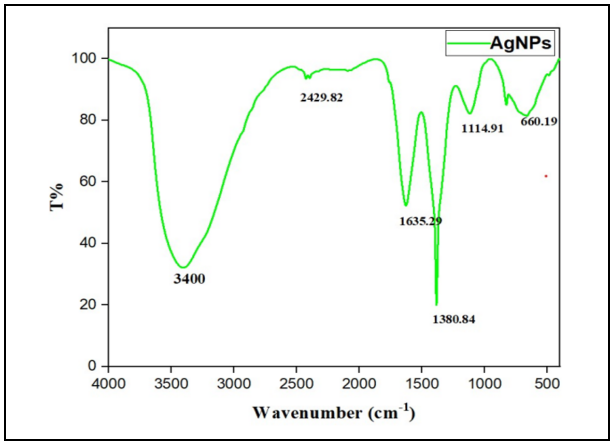

Fig. 4: FTIR characterization of the synthesized AgNPs

Fig. 5 shows the XRD characterization of the synthesized AgNPs. It is a reliable technique for determining phase composition and degree of crystallinity (Amin *et al.* 2026). The diffraction pattern showed characteristic peaks at 2θ values of 27.61˚, 32.02˚, 37.93˚, 46.08˚, 54.7˚, and 76.67˚, indexed to the (111), (200), (220), (311), (222), and (400) planes, respectively. A similar study reported well-defined diffraction peaks at approximately 38°, 44°, 64°, and 77°, corresponding to the (111), (200), (220), and (311) crystallographic planes, respectively, confirming the face-centered cubic (FCC) structure and crystalline phase of the synthesized AgNPs (Sheeba *et al.* 2024; Rashed *et al.* 2025). Rashed *et al.* (2025) further reported distinct diffraction peaks at 2θ values of 38.139°, 44.26°, 64.51°, and 77.40° for the untreated sample, while the microwave-treated sample exhibited peaks at 32.17°, 38.098°, 44.26°, 46.14°, 64.45°, and 77.40°. The peaks at approximately 38.10°, 44.26°, 64.45°, and 77.40° were assigned to the (111), (200), (220), and (311) planes, respectively, in agreement with JCPDS Card No. 04-0783.

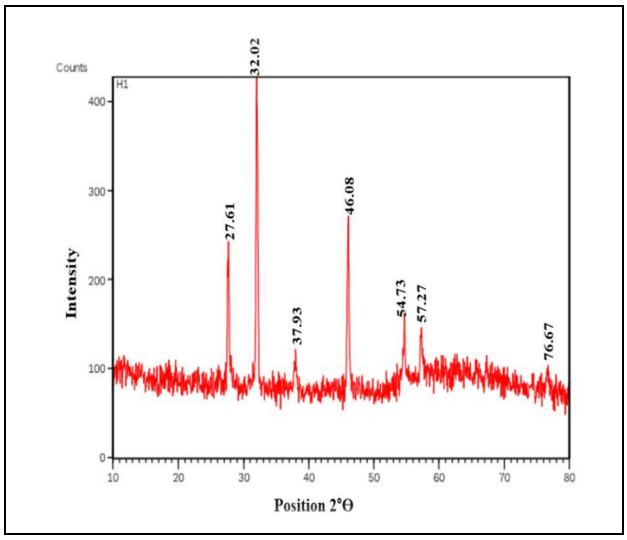

Fig. 5: XRD characterization of the synthesized AgNPs

AgNPs mediated by *Manilkara zapota* and *Curcuma longa* exhibit a wide spectrum of therapeutic applications, particularly antioxidant, anti-inflammatory, and antimicrobial effects. Oxidative stress results from an imbalance between the cell's antioxidative defense system and oxidants (Bedlovičová *et al.* 2020). Antioxidants act as counteragents to oxidants; they can be natural or synthetic agents that mitigate ROS-induced oxidative damage (Azeez *et al.* 2017; Dilipan *et al.* 2023).

In this study, the antioxidant activity of AgNPs was assessed by DPPH, H_2O_2, FRAP, ABTS, and NO assays. DPPH assay (Fig. 6A) demonstrated a concentration-dependent increase in free-radical scavenging activity. At concentrations ranging from 10 to 50 µg/mL, the inhibition values were 41 ± 1.5%, 53 ± 2%, 66 ± 3%, 77 ± 3%, and 86 ± 3%, respectively, with the highest inhibition observed at the highest concentration. The synthesized AgNPs exhibited an IC_{50} value of 12.5 µg/mL, compared with 16.7 µg/mL for the standard ascorbic acid, indicating comparable antioxidant activity. H_2O_2 scavenging assay (Fig. 6B) demonstrated a marked increase in inhibition with increasing concentration. The *M. zapota*- and *C. longa*-mediated AgNPs showed inhibition values of 48 ± 2%, 55 ± 2.1%, 72 ± 3%, 73 ± 3%, and 84 ± 4% at concentrations of 10, 20, 30, 40, and 50 µg/mL, respectively, with an IC_{50} value of 13.3 µg/mL. The standard ascorbic acid showed marginally higher antioxidant activity than the AgNP formulation. At higher concentrations, the percentage inhibition increased and approached that of the standard, with an IC_{50} value of 8.3 µg/mL.

The FRAP assay (Fig. 6C) of the synthesized AgNPs showed a consistent, concentration-dependent increase in antioxidant activity, nearly comparable to the standard across concentrations. The inhibition values were 54 ± 3%, 65 ± 3%, 72 ± 4%, 76 ± 4%, and 81 ± 4% at concentrations of 10, 20, 30, 40, and 50 µg/mL, respectively, with an IC_{50} value of 9.3 µg/mL, whereas the standard antioxidant exhibited an IC_{50} value of 8.6 µg/mL (Fig. 6C).

The ABTS assay (Fig. 6D) confirmed a concentration-dependent increase in inhibitory activity from 10 to 50 µg/mL for both the standard and green-synthesized AgNPs. The AgNPs showed inhibition values of 53 ± 3%, 60 ± 3%, 68 ± 4%, 74 ± 4%, and 83 ± 4%, respectively, with an IC_{50} of 9.4 µg/mL. The standard ascorbic acid showed marginally higher inhibition (85.34%), with an IC_{50} of 8.8 µg/mL.

Similarly, the nitric oxide scavenging assay (Fig. 6E) showed a progressive increase in scavenging activity for both the standard and synthesized AgNPs as the concentration increased from 10 to 50 µg/mL. The AgNPs showed inhibition values of 56 ± 3%, 63 ± 3%,

72 ± 3%, 75 ± 4%, and 80 ± 4%, respectively, with an IC_{50} of 8.9 µg/mL, whereas the standard showed an IC_{50} of 8.3 µg/mL. Overall, the green-synthesized AgNPs demonstrated promising antioxidant activity across the tested assays (Figs. 6A–E).

Salari *et al.* (2019) reported that green-synthesized AgNPs demonstrated dose-dependent antioxidant activity, with inhibition increasing from 43.39% to 63.56% at concentrations ranging from 0.2 to 1.0 mg/mL, with an IC_{50} value of 0.70 ± 0.08 µg/mL, compared with the plant extract (1.64 ± 0.09) and standard ascorbic acid (0.26 ± 0.09) mg/mL. Similarly, a study on *Tinospora cordifolia*-mediated AgNPs reported concentration-dependent antioxidant activity, with inhibition values of 10, 18, 22, and 31% at concentrations of 25, 50, 75, and 100 µg/mL, respectively (Lekkala *et al.* 2025).

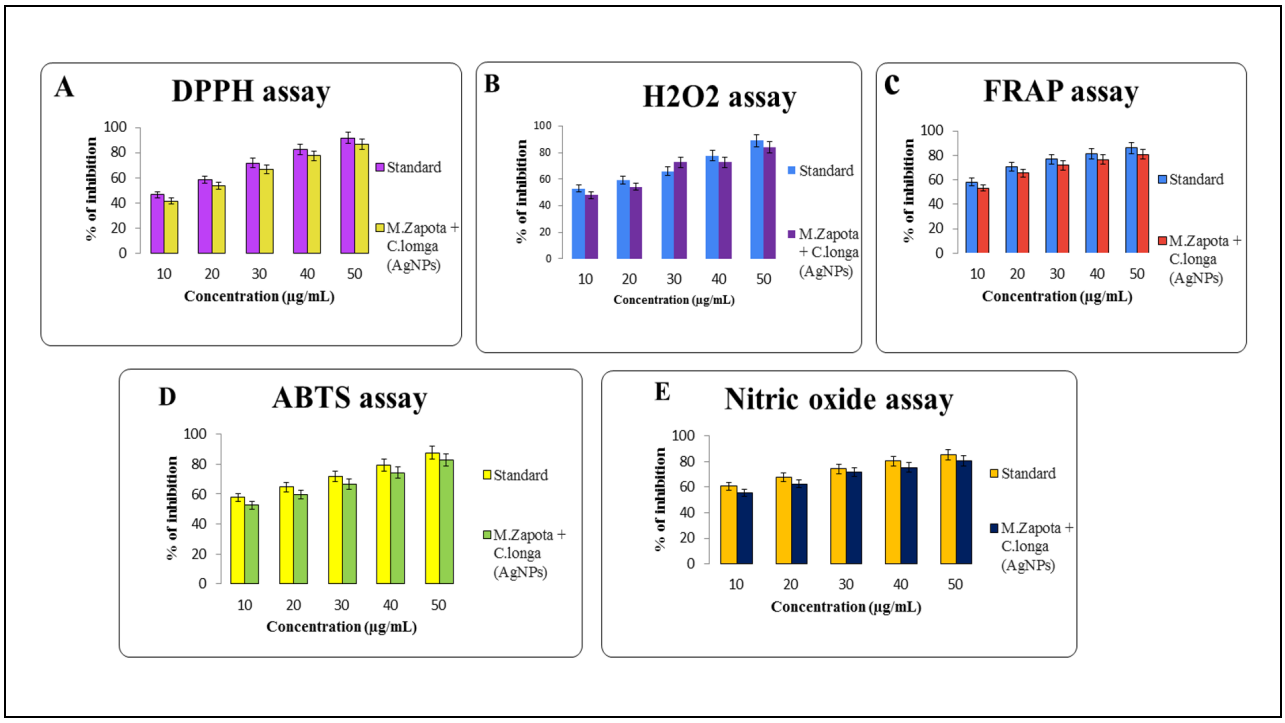

Fig. 6: Antioxidant activity of biologically synthesized AgNPs: (A) DPPH, (B) H_2O_2, (C) FRAP, (D) ABTS, and (E) NO assays

Protein denaturation is one of the processes associated with inflammation. Therefore, the anti-inflammatory activity of the synthesized AgNPs was evaluated using BSA, egg albumin (EA), and MSA assays. The BSA assay results demonstrated a concentration-dependent increase in protein-denaturation inhibitory activity for both the standard and AgNPs. Compared with standard diclofenac sodium, the *M. zapota*- and *C. longa*-mediated AgNPs showed potent protein-stabilizing activity with a closely parallel pattern, reaching 78.32% inhibition at 50 µg/mL, comparable to that of standard diclofenac sodium (Fig. 7A). The BSA assay exhibited inhibition values of 41 ± 2%, 53 ± 3%, 65 ± 3%, 72 ± 3%, and 79 ± 4% at concentrations of 10, 20, 30, 40, and 50 µg/mL, respectively, with an IC_{50} value of 18.3 µg/mL, whereas the standard diclofenac sodium showed an IC_{50} value of 14.2 µg/mL.

The EA assay (Fig. 7B) showed a progressive increase in inhibition with increasing concentration. The *M. zapota*- and *C. longa*-mediated AgNPs exhibited inhibition values of 50 ± 2%, 55 ± 3%, 62 ± 3%, 67 ± 3%, and 76 ± 4% at concentrations of 10, 20, 30, 40, and 50 µg/mL, respectively, with an IC_{50} value of 10.0 µg/mL, whereas the standard exhibited an IC_{50} value of 9.4 µg/mL.

Similarly, the MSA assay demonstrated a concentration-dependent increase in inhibition (Fig. 7C). The AgNPs showed inhibition values of 54 ± 2%, 60 ± 3%, 72 ± 3%, 77 ± 3%, and 83 ± 4% at concentrations of 10, 20, 30, 40, and 50 µg/mL, respectively, with an IC_{50} value of 9.3 µg/mL, while the standard exhibited an IC_{50} value of 8.8 µg/mL.

The findings are consistent with previous reports. Jeon *et al.* (2024) reported that green-synthesized AgNPs using black mulberry exhibited protein-denaturation inhibition of 4.21%, 6.52%, 7.81%, and 14.52% at concentrations of 10, 50, 100, and 250 µg/mL, respectively. They reported that environmentally friendly AgNPs synthesized using *Zingiber officinale* and *Ocimum gratissimum* formulations showed 78% inhibition at 50 µg/mL, compared with the standard diclofenac sodium. Another study reported that AgNPs synthesized using *Z. officinale* and *O. gratissimum*

formulations showed a maximum inhibition of 74% at 50 µg/mL compared with standard diclofenac sodium. Similarly, AgNPs synthesized using *O. tenuiflorum* and *O. gratissimum* herbal formulations exhibited maximum inhibition of 75% at 50 µg/mL, compared with 81% for standard diclofenac sodium. A further study reported concentration-dependent inhibition by biosynthesized AgNPs from arrowroot, with the highest inhibition at 50 µg/mL (Krishna *et al.* 2025).

In the present study, the MSA assay confirmed a concentration-dependent enhancement in protein-denaturation inhibition, with maximum inhibition of 83% at 50 µg/mL. This suggests a potential ability of the AgNPs to stabilize the RBC membrane. The activity of the AgNPs was closely comparable to that of the standard drug diclofenac sodium (Fig. 7C). A previous study reported that green-synthesized AgNPs using leaf extracts of *Guazuma ulmifolia* Lam. showed maximum inhibition of 73.27 ± 0.89% at 1000 µg/mL, compared with 85.32 ± 0.84% inhibition for standard aspirin (Santhanakumar *et al.* 2024).

The antimicrobial activity of AgNPs against *E. coli*, *E. faecium*, *Pseudomonas* sp., *S. aureus*, and *C. albicans* showed a concentration-dependent inhibition pattern. Fig. 8 shows that the synthesized AgNPs generally exhibited increased antimicrobial activity with increasing concentration. For *E. coli*, the inhibition zone increased from 14 mm at 25 µg/mL to 18 mm at 50 µg/mL, whereas the standard amoxicillin produced an inhibition zone of 38 mm at 20 µg/mL. Against *Pseudomonas* sp., inhibition zones of 18, 19, and 20 mm were recorded at 25, 50, and 100 µg/mL, respectively, while the standard showed an inhibition zone of 33 mm at 20 µg/mL.

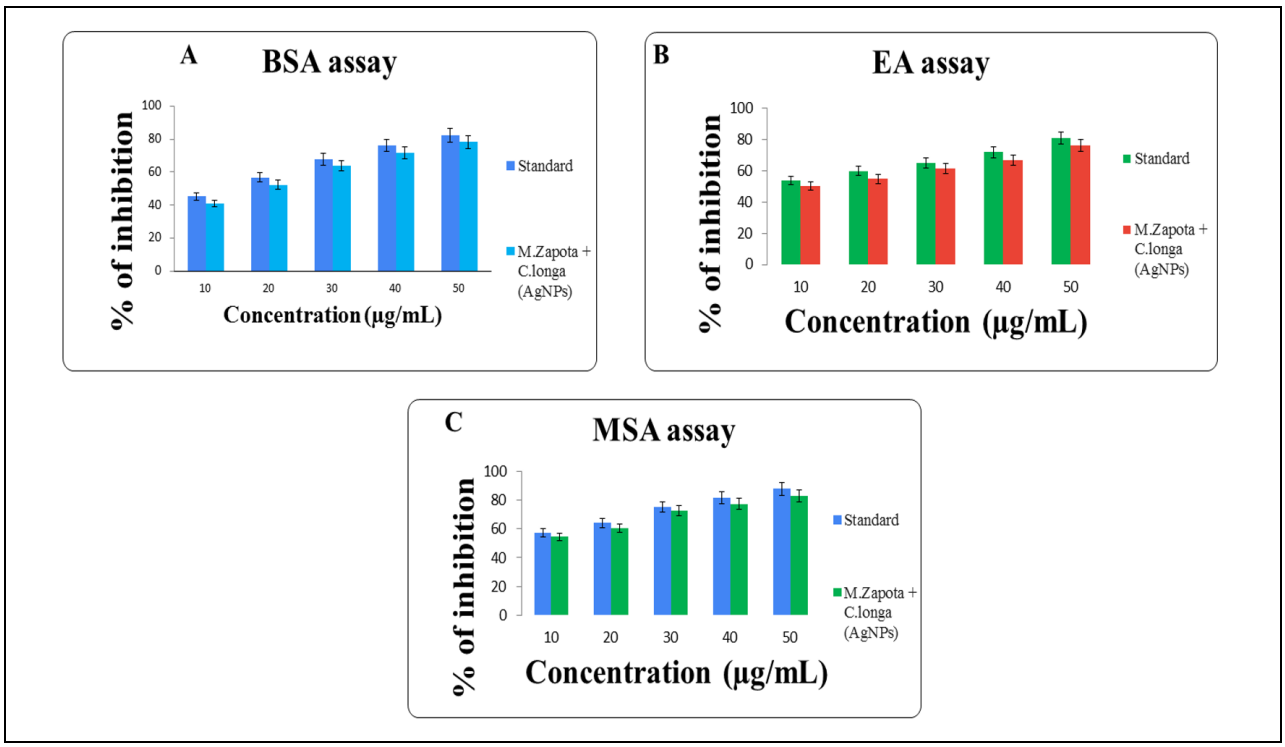

Fig. 7: Anti-inflammatory activity of the synthesized AgNPs: (A) BSA, (B) EA, and (C) MSA assays

For *E. faecium*, the AgNPs produced inhibition zones of 16, 17, and 39 mm at 25, 50, and 100 µg/mL, respectively, which approached the standard inhibition zone of 41 mm. The antimicrobial activity against *S. aureus* also demonstrated a concentration-dependent effect, with inhibition zones of 20, 20, and 21 mm at 25, 50, and 100 µg/mL, respectively. The standard showed a 40 mm inhibition zone at 20 µg/mL. The *M. zapota*- and *C. longa*-mediated AgNPs also exhibited antimicrobial activity against *C. albicans*, with inhibition zones of 9, 12, and 12 mm at 25, 50, and 100 µg/mL, respectively. The standard fluconazole showed superior activity, with a 40 mm inhibition zone at 20 µg/mL.

Recent findings reported that biologically synthesized AgNPs produced inhibition zones of 13.53 ± 0.32 mm against *E. coli* and 13.36 ± 0.70 mm against *S. aureus*. Furthermore, the inhibition zone increased to 14.40 ± 0.37 mm with ciprofloxacin-conjugated AgNPs, highlighting a possible synergistic effect (Din *et al.*, 2024). *Tinospora cordifolia*-mediated AgNPs reportedly produced a 37 mm inhibition zone against *E. coli* at 100 µg/mL, using ciprofloxacin (5 µg) as the standard antibiotic (Lekkala *et al.* 2025). Another study reported that AgNPs synthesized using *O. tenuiflorum* and *O. gratissimum* herbal formulations showed significant antibacterial activity against *Streptococcus mutans*,

Staphylococcus aureus, *Enterococcus faecalis*, and *Lactobacillus* sp., even at low concentrations of 25 µg/mL. Similar activity was observed against *C. albicans*, while the 5-h time–kill curve assay showed a time-related reduction in microbial growth. Tharani *et al.* (2023) reported the inhibitory potential of AgNPs against *Pseudomonas* sp., *S. aureus*, and *E. coli* at concentrations ranging from 10 to 1000 µg/mL, demonstrating enhanced bactericidal effects using the agar-well diffusion method.

The time–kill curve assay further demonstrated concentration- and time-dependent antimicrobial efficacy of the green-synthesized AgNPs against the tested microorganisms.

As shown in Fig. 9, treatment with AgNPs at 100 µg/mL for 4 h reduced the *S. aureus* count from 7.15 to 3.71 $\log_{10}$ CFU/mL, corresponding to a 3.44-log reduction. Similarly, *Pseudomonas* sp. showed a decline from 7.11 to 3.97 $\log_{10}$ CFU/mL, corresponding to a 3.14-log reduction, while *E. faecium* showed a reduction from 6.45 to 3.67 $\log_{10}$ CFU/mL, corresponding to a 2.78-log reduction. *C. albicans* decreased from 4.55 to 2.51 $\log_{10}$ CFU/mL, corresponding to a 2.04-log reduction. The untreated control showed no significant reduction, whereas the AgNP-treated groups showed a significant reduction in microbial counts ($p < 0.05$). Nevertheless, the standard antibiotic remained slightly more effective.

A recent study reported that *Plectranthus amboinicus*-mediated AgNPs produced a concentration- and time-dependent inhibition zone of 13.53 ± 0.32 mm against *E. coli*, with complete inhibition reported at 100 µg/mL, whereas 25 and 50 µg/mL showed lower but progressive inhibition (Dibua and Ezeh, 2025). Similarly, garlic-derived AgNPs showed antibacterial activity against wound pathogens, including *Escherichia fergusonii*, while the synergistic treatment of AgNPs and ciprofloxacin resulted in a 3-$\log_{10}$ CFU/mL reduction within 24 h (Abdelkhalig *et al.* 2025).

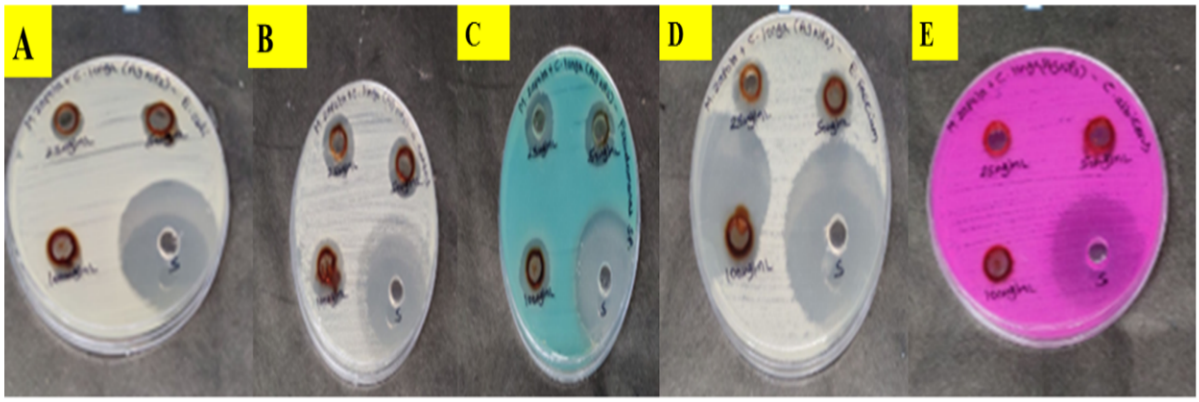

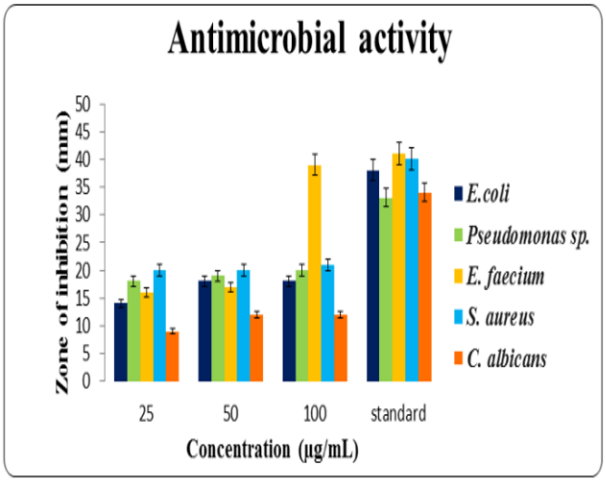

Fig. 8: Antimicrobial activity of synthesized AgNPs by agar well diffusion assay against (A) *E. coli*, (B) *E. faecium*, (C) *Pseudomonas* sp., (D) *S. aureus*, and (E) *C. albicans*

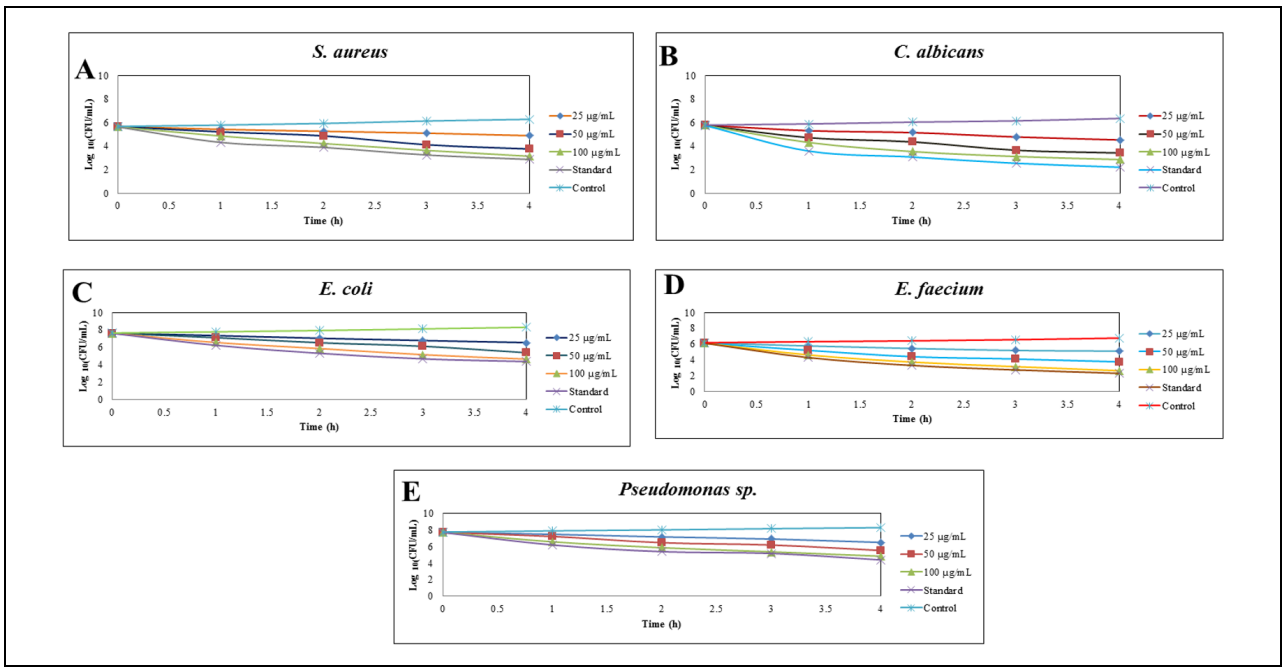

Fig. 9: Time–kill curve analysis of AgNPs against (A) *S. aureus*, (B) *C. albicans*, (C) *E. coli*, (D) *E. faecium*, and (E) *Pseudomonas* sp.

The brine shrimp lethality assay demonstrated that *M. zapota*- and *C. longa*-mediated AgNPs, at concentrations ranging from 5 to 80 µg/mL, showed high viability of nauplii on both days 1 and 2 (Fig. 10). No substantial mortality was observed even at the highest concentration, indicating low acute toxicity of the nanoparticles under the tested conditions. A similar study reported that green-synthesized *Plectranthus amboinicus*-mediated AgNPs caused dose-dependent mortality (Supriya *et al.* 2025). *Nigella sativa*-mediated AgNPs demonstrated minimal cytotoxicity, with an LC_{50} value of 1000.91 µg/mL (Dibua and Ezeh, 2025).

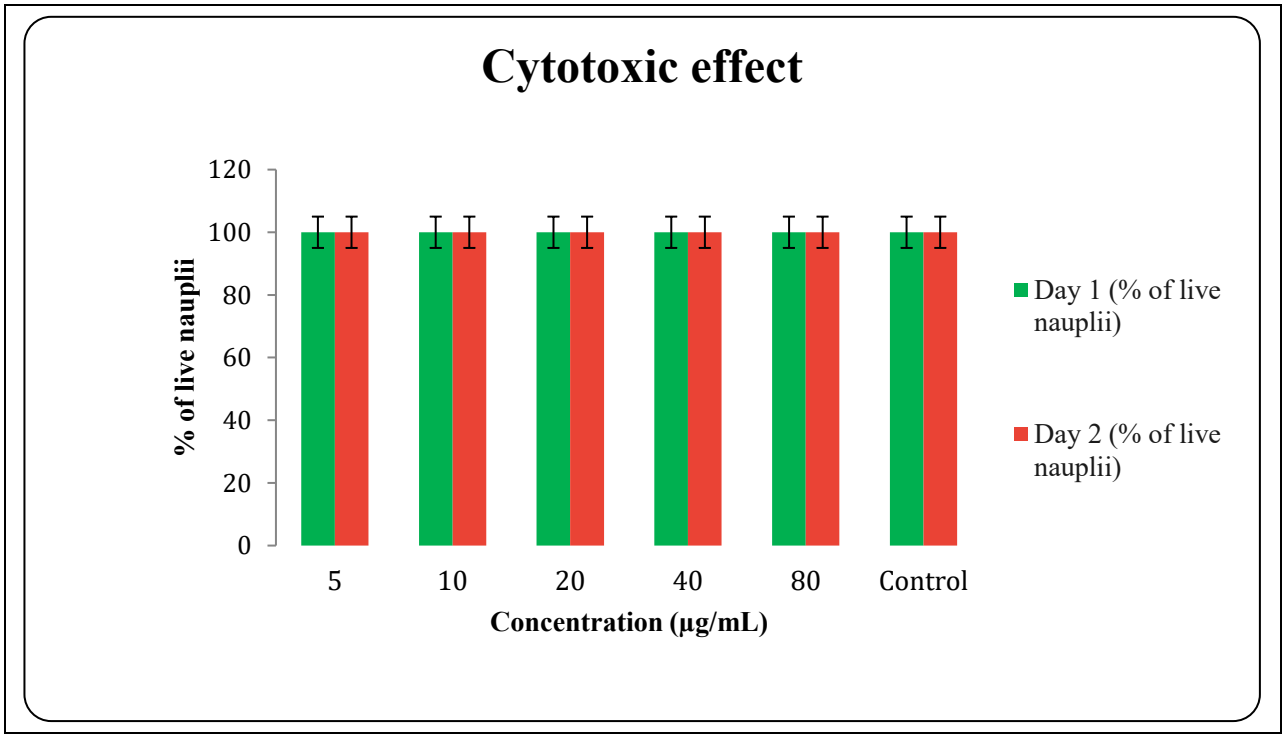

Fig. 10: Cytotoxicity of synthesized AgNPs using the brine shrimp lethality assay

5. CONCLUSION

The present work highlights the eco-friendly synthesis of AgNPs mediated by *M. zapota* and *C. longa* herbal formulations. The synthesized AgNPs exhibited a characteristic UV–Vis absorption peak at 435 nm, while SEM analysis showed predominantly spherical nanoparticles with an average particle size of 16.12 nm. FTIR and XRD analyses indicated the presence of phytochemical functional groups and the crystalline nature of the synthesized AgNPs, respectively, and demonstrated concentration-dependent antioxidant activity, protein-denaturation inhibitory activity, and enhanced antimicrobial activity against the tested microorganisms. The time–kill assay further demonstrated concentration- and time-dependent inhibition, and the cytotoxicity study showed minimal toxicity under the tested conditions. While the findings are promising, this study is limited to *in vitro* analysis; future studies including minimum inhibitory concentration (MIC), minimum bactericidal concentration (MBC), mammalian cell studies, and wound-healing assays are crucial to validate the therapeutic potential.

ABBREVIATIONS

AgNPs – Silver nanoparticles

DPPH – 2,2-Diphenyl-1-picrylhydrazyl

H_2O_2 – Hydrogen peroxide

FRAP – Ferric reducing antioxidant power

NO – Nitric oxide

BSA – Bovine serum albumin

MSA – Membrane stabilization assay

ABTS – 2,2′-Azino-bis(3-ethylbenzothiazoline-6-sulfonic acid)

ACKNOWLEDGEMENTS

The authors are thankful to Saveetha Medical College and Hospital, Saveetha Institute of Medical and Technical Sciences, Saveetha University, Chennai, TN, India, for providing the necessary facilities and support to carry out this study.

AUTHOR CONTRIBUTIONS

The study framework and conceptual framework were formulated by Rajeshkumar Shanmugam. Steffy Dominic conducted data collection and documentation. Data evaluation and validation of the findings were collectively performed by Steffy Dominic, Perumal Elumalai, Rajeshkumar Shanmugam, and Nalini Jeyaprakash. The preliminary manuscript was written by Rajeshkumar Shanmugam and Steffy Dominic. All authors assessed the results and approved the finalized manuscript.

FUNDING

This research received no specific grant from any funding agency in the public, commercial, or not-for-profit sectors.

CONFLICTS OF INTEREST

The authors declare that there is no conflict of interest.

COPYRIGHT

This article is an open-access article distributed under the terms and conditions of the Creative Commons Attribution (CC BY) license (http://creativecommons.org/licenses/by/4.0/).

REFERENCES

Abdelkhalig, S. M., Ali, A. G., Ghaly, M. F., Alharbi, N. K., Alharbi, M., Bendary, M. M. and Abousaty, A. I., Eco-friendly silver nanoparticles from garlic: a novel therapeutic approach for treating *Escherichia fergusonii* wound infections. Frontiers in Cellular and Infection, *Microbio*., 15, 1604507 (2025). https://doi.org/10.3389/fcimb.2025.1604507

Abdulsahib, S. S., Synthesis, characterization and biomedical applications of silver nanoparticles, *Biomed.,* 41(2), 458-464 (2021). https://doi.org/10.51248/.v41i2.1058

Ahmed, S., Ahmad, M., Swami, B. L. and Ikram, S., A review on plants extract mediated synthesis of silver nanoparticles for antimicrobial applications: a green expertise, *J. Adv. Res.,* 7(1), 17-28 (2016). https://doi.org/10.1016/j.jare.2015.02.007

Alsareii, S. A., Alzerwi, N. A., Alasmari, M. Y., Alamri, A. M., Mahnashi, M. H., Shaikh, I. A., Savant, C., Kulkarni, P. V., Shettar, A. K., Hoskeri, J. H. and Kumbar, V., *Manilkara zapota* L. extract topical ointment application to skin wounds in rats speeds up the healing process, *Front. Pharmacol*., 14, 1206438 (2023). https://doi.org/10.3389/fphar.2023.1206438

Amin, D. S., Banu, A. N. and Mishra, J., *Curcuma longa*-mediated Biogenic and Eco-friendly Silver Nanoparticles with Promising Antibacterial Activity, *J. Pure Appl. Microbio*., 20(1), 622 (2026). https://doi.org/10.22207/JPAM.20.1.48

Azeez, L., Lateef, A. and Adebisi, S. A., Silver nanoparticles (AgNPs) biosynthesized using pod extract of Cola nitida enhances antioxidant activity and phytochemical composition of Amaranthus caudatus Linn, *Appl. Nanosci*., 7(1-2), 59-66 (2017). https://doi.org/10.1007/s13204-017-0546-2

Balan, K., Qing, W., Wang, Y., Liu, X., Palvannan, T., Wang, Y., Ma, F. and Zhang, Y., Antidiabetic activity of silver nanoparticles from green synthesis using Lonicera japonica leaf extract, *RSC Adv*., 6(46), 40162-40168 (2016). https://doi.org/10.1039/c5ra24391b

Bedlovičová, Z., Strapáč, I., Baláž, M. and Salayová, A., A brief overview on antioxidant activity determination of silver nanoparticles, *Mol.*, 25(14), 3191 (2020). https://doi:10.3390/molecules25143191

Chainani-Wu, N., Safety and anti-inflammatory activity of curcumin: a component of tumeric (*Curcuma longa*), *J. Alternat. Complement. Med.*, 9(1), 161-168 (2003). https://doi.org/10.1089/107555303321223035

Choi, Y., Kim, W., Lee, J. S., Youn, S. J., Lee, H. and Baik, M. Y., Enhanced antioxidant capacity of puffed turmeric (*Curcuma longa* L.) by high hydrostatic pressure extraction (HHPE) of bioactive compounds, *Foods,* 9(11), 1690 (2020). https://doi.org/10.3390/foods9111690

Dhanapal, P., Shanmugam, R., Lingaraj, J. and Pradeep, M., *Ocimum gratissimum* mediated synthesis of AgNPs–An in vitro analysis of anti-inflammatory and antimicrobial effects, *Med. J. Malaysia*, 80(1), 1-6 (2025).

Dibua, M. E. and Ezeh, C. K., Evaluation of Cytotoxicity of Nigella sativa-Mediated Silver Nanoparticles Using Brine Shrimp Lethality Assay, *J. Pharmacol. Pharma. Res.,* 2(4), 179-184 (2025). https://doi.org/10.5455/JPPR.20250725014124

Dilipan, E., Sivaperumal, P., Kamala, K., Ramachandran, M. and Vivekanandhan, P., Green synthesis of silver nanoparticles using seagrass Cymodocea serrulata (R. Br.) Asch. & Magnus, characterization, and evaluation of anticancer, antioxidant, and antiglycemic index, *Biotechnol. Appl. Biochem.,* 70(3), 1346-1356 (2023). https://doi.org/10.1002/bab.2444

Din, U. M. M., Batool, A., Ashraf, R. S., Yaqub, A., Rashid, A. and Din, N. M., Green synthesis and characterization of biologically synthesized and antibiotic-conjugated silver nanoparticles followed by post-synthesis assessment for antibacterial and antioxidant applications, *ACS omega*, 9(17), 18909-18921 (2024). https://doi.org/10.1021/acsomega.3c08927

Gomathy, K., Baskar, R. and Kumaresan, K., Comparison of antioxidant potential in pulp and peel extracts of *Manilkara zapota* (L.) P. Royen, *Afr. J. Biotechnol.*, 12(31), 4936-4943 (2013). https://doi.org/10.5897/AJB2012.2961

Grover, M., Behl, T., Sehgal, A., Singh, S., Sharma, N., Virmani, T., Mahesh, R., Farasani, A., Sridevi, C., Amal, A. M., Ghazi, F. S., Mohit, S. and Simona, B., In Vitro Phytochemical Screening, Cytotoxicity Studies of *Curcuma longa* Extracts with Isolation and Characterisation of Their Isolated Compounds, *Mol.,* 26(24), 7509 (2021). https://doi.org/10.3390/molecules26247509

Iravani, S., Korbekandi, H., Mirmohammadi, S. V. and Zolfaghari, B., Synthesis of silver nanoparticles: chemical, physical and biological methods, *Res. Pharma. Sci.,* 9(6), 385-406 (2014).

Jeon, Y. N., Ryu, S. J., Lee, H. Y., Kim, J. O. and Baek, J. S., Green synthesis of silver nanoparticle using black mulberry and characterization, phytochemical, and bioactivity, *Antibio.*, 13(8), 686 (2024). https://doi.org/10.3390/antibiotics13080686

Joshi, P., Pandey, L., Patel, A., Baksh, Z., Singh, P., Singh, R., Green Synthesis and Characterization of Silver Nanoparticles Using *Stachytarpheta indica*, *Int. J. Current Microbio. Appl. Sci*., 14(4), 16-24 (2025). https://doi.org/10.20546/ijcmas.2025.1404.004

Khan, I., Saeed, K. and Khan, I., Nanoparticles: Properties, applications and toxicities, *Arab. J. Chem.,* 12(7), 908-931 (2019). https://doi.org/10.1016/j.arabjc.2017.05.011

Krishna, S., Bhaskaran, R. and Kumar, S. P., Evaluating the Anti-Oxidant Properties of Arrow Root Extract Silver Nanoparticles-An Invitro Study, *Cuestiones de Fisioterapia*, 54(4), 6653-6663 (2025). https://doi.org/10.48047/jf1x2t66

Lekkala, V. D., Muktinutalapati, A. V., Lebaka, V. R., Lomada, D., Korivi, M., Li, W. and Reddy, M. C., Green synthesis and characterization of silver nanoparticles from *Tinospora cordifolia* leaf extract:Evaluation of their antioxidant, anti-inflammatory, antibacterial, and antibiofilm efficacies, *Nanomater.*, 15(5), 381 (2025). https://doi.org/10.3390/nano15050381

Li, H. and Li, Y., Network pharmacology analysis of molecular mechanism of *Curcuma longa* L. Extracts regulating glioma immune inflammatory factors: implications for precise cancer treatment, *Curr. Topics Med. Chem.,* 22(4), 259-267 (2022). https://doi.org/10.2174/1568026621666210910123749

Li, Y., Liao, Q., Hou, W. and Qin, L., Silver-based surface plasmon sensors: fabrication and applications, *Int. J. Mol. Sci*., 24(4), 4142 (2023). https://doi.org/10.3390/ijms24044142

Majani, S. S., Ramesh, K. B., Devendra, B. K., Sridhara, S. P. B., Singh, P., Iqbal, M., Abass, K. S., Shivamallu, C., Amachawadi, R. G., Stupin, V. and Silina, E., Bio-combustion synthesis of silver nanoparticles and evaluation of their effective antibacterial and photodegradation properties, *Sci. Rep.,* 16, 2316 (2025). https://doi.org/10.1038/s41598-025-32173-w

Parashar, S. and Garg, M., Optimized green synthesis of *Manilkara zapota* capped silver nanoparticles and their antimicrobial application through formulation of nano-gel systems, *Nano Biomed. Eng*., 15(3), 262-277 (2023). https://doi.org/10.26599/NBE.2023.9290020

Pauline, C. R., Akshita, Pavithra, T., Kannan, K. and Sivaperumal, P., Characterization and biological activity of silver nanoparticles from (Rhizophora Mucronata) mangrove extract, *Nano Life*., 15(03), 2450018 (2025). https://doi.org/10.1142/S1793984424500181

Rashed, M. N., Abdelrady, E. and Ghabrial, T. M., Microwave assisted green synthesis of silver nanoparticles using Trigonella Hamosa L. plant extract for the photodegradation of some water pollutants, *Sci. Rep.,* 15(1), 37344 (2025). https://doi.org/10.1038/s41598-025-21112-4

Rivas-Gastelum, M. F., Garcia-Amezquita, L. E., Garcia-Varela, R. and Sánchez-López, A. L., *Manilkara zapota* "chicozapote" as a fruit source of health-beneficial bioactive compounds and its effects on chronic degenerative and infectious diseases, a review, *Front. Nutri*., 10, 1194283 (2023). https://doi.org/10.3389/fnut.2023.1194283

Rizwana, H., Alwhibi, M. S., Al-Judaie, R. A., Aldehaish, H. A. and Alsaggabi, N. S., Sunlight-mediated green synthesis of silver nanoparticles using the berries of Ribes rubrum (red currants): characterisation and evaluation of their antifungal and antibacterial activities, *Mol.,* 27(7), 2186 (2022). https://doi.org/10.3390/molecules27072186

Sagar, P. V. P. S. R., Ramadevi, D., Basavaiah, K. and Botsa, S. M., Green synthesis of silver nanoparticles using aqueous leaf extract of *Saussurea obvallata* for efficient catalytic reduction of nitrophenol, antioxidant, and antibacterial activity, *Water Sci. Eng.*, 17(3), 274-282 (2024). https://doi.org/10.1016/j.wse.2023.09.004

Sahu, K., Kurrey, R. and Pillai, A. K., Green synthesis of silver nanoparticles from *Manilkara zapota* leaf extract for the detection of aminoglycoside antibiotics and other applications, *RSC Adv*., 14(32), 23240-23256 (2024). https://doi.org/10.1039/d4ra01906g

Salari, S., Bahabadi, S. E., Samzadeh-Kermani, A. and Yosefzaei, F., In-vitro evaluation of antioxidant and antibacterial potential of greensynthesized silver nanoparticles using Prosopis farcta fruit extract, *Iran. J. Pharma. Res*., 18(1), 430-445 (2019). https://doi.org/10.22037/ijpr.2019.2330

Santhanakumar, C., Vanitha, A., Saralabai, V. C. and Kalimuthu, K., Natural Green Synthesis of Silver Nanoparticles Using Leaf Extract of *Guazuma Ulmifolia* Lam. And Analysis of Its Antimicrobial, Anti-Inflammatory and Anticancer Activities, *Int. J. Pharma. Sci. Drug Res.,* 16(5), 813-824 (2024). https://doi.org/10.25004/IJPSDR.2024.16050

Segneanu, A. E., Vlase, G., Lukinich-Gruia, A. T., Herea, D. D. and Grozescu, I., Untargeted metabolomic approach of *Curcuma longa* to neurodegenerative phytocarrier system based on silver nanoparticles, *Antioxi.,* 11(11), 2261 (2022). https://doi.org/10.3390/antiox11112261

Selvan, D. A., Mahendiran, D., Kumar, R. S. and Rahiman, A. K., Garlic, green tea and turmeric extracts-mediated green synthesis of silver nanoparticles: Phytochemical, antioxidant and in vitro cytotoxicity studies, *J. Photochem. Photobio. B: Bio.,* 180, 243-252 (2018). https://doi.org/10.1016/j.jphotobiol.2018.02.014

Shahraki, R. Z., Shokoohizadeh, L., Chegini, Z., Sharifi, E. and Arabestani, M. R., Antibacterial and antibiofilm activities of curcumin-mediated green-synthesised silver nanoparticles against Methicillin-resistant *Staphylococcus aureus* and *Pseudomonas aeruginosa*, *BMC Biotechnol*., 26(1), 75 (2026). https://doi.org/10.1186/s12896-026-01138-w

Sharifi-Rad, J., Rayess, Y. E., Rizk, A. A., Sadaka, C., Zgheib, R., Zam, W., Sestito, S., Rapposelli, S., Neffe-Skocińska, K., Zielińska, D., Salehi, B., William, S. N., Noura, D. S., Taheri, Y., Marc, E. B., Miquel, M., Adrian, O. E., Ansar, S. H. R., Cho, W. C., Alfred, M. and Natalia, M., Turmeric and its major compound curcumin on health: bioactive effects and safety profiles for food, pharmaceutical, biotechnological and medicinal applications, *Front. Pharmacol.,* 11, 01021 (2020). https://doi.org/10.3389/fphar.2020.01021

Sheeba, N. L. and Sundar, S. M., Critical evaluation of silver nanoparticles synthesized at room temperature/microwave irradiation: A green approach, *Next Nanotechnol*., 6, 100083 (2024). https://doi.org/10.1016/j.nxnano.2024.100083

Singh, R. and Lillard, J. J., Nanoparticle-based targeted drug delivery, *Exp. Mol. Pathol.,* 86(3), 215-223 (2009). https://doi.org/10.1016/j.yexmp.2008.12.004

Subedi, T., A study on the medicinal chemistry of *Curcuma longa*, *Himalayan Biodivers*., 7(1), 39-46 (2019). https://doi.org/10.3126/hebids.v7i1.40188

Supriya, Y., Munusamy, T. and Sivamalar, S., Green-synthesized Plectranthus amboinicus silver nanoparticles with broad-spectrum biological activities, *Discover Biotechnol.,* 2(1), 30 (2025). https://doi.org/10.1007/s44340-025-00041-y

Tharani, M., Rajeshkumar, S., Al-Ghanim, K. A., Nicoletti, M., Sachivkina, N. and Govindarajan, M., Terminalia chebula-assisted silver nanoparticles: biological potential, synthesis, characterization, and ecotoxicity, *Biomed.*, 11(5), 1472 (2023). https://doi.org/10.3390/biomedicines11051472

Varadharajan, S. and Pandian, P., Antioxidant, Antimicrobial, and Potential Biomedical Applications of Green Synthesized Silver Nanoparticles Using Aloe barbadensis Root, *J. Environ. Nanotechnol.,* 14(1), 97-103 (2025). https://doi.org/10.13074/jent.2025.03.2511226

Varghese, R. E., Ragavan, D., Sivaraj, S., Gayathri, D. and Kannayiram, G., Anti-inflammatory activity of Syzygium Aromaticum silver nanoparticles: In vitro and in silico study, *Asian J. Pharm. Clin. Res*., 10(11), 370-373 (2017). https://doi.org/10.22159/ajpcr.2017.v10i11.19904

Wickenberg, J., Ingemansson, S. L. and Hlebowicz, J., Effects of *Curcuma longa* (turmeric) on postprandial plasma glucose and insulin in healthy subjects, *Nutri. J.,* 9(1), 43 (2010). https://doi.org/10.1186/1475-2891-9-43